Article
Vol. 26, No. 3, p. 349–365, June 2022
https://doi.org/10.1007/s12303-021-0035-1
pISSN 1226-4806 eISSN 1598-7477
Geosciences Journal GJ

Geochemical characteristics and origins of hydrocarbon gases in the shallow gas field in the Pohang Basin, Korea

Jiyoung Choi[1]*, Nyeon-Keon Kang[1], In Gul Hwang[1], and Dong-Hun Lee[2]

[1]Oil and Gas Research Center, Petroleum and Marine Research Division, Korea Institute of Geoscience and Mineral Resources (KIGAM), 124 Gwahak-ro, Yuseong-gu, Daejeon 34132, Republic of Korea
[2]Marine Environment Research Division, National Institute of Fisheries Science, 46083 Busan, Republic of Korea

ABSTRACT: The shallow biogenic gas system of the Pohang Basin (Miocene) in Korea is examined by analyzing organic matter (amount, type, and maturity) of bulk rocks and hydrocarbons (molecular and isotopic signatures) in the dissolved and void gases obtained from five wells. The high organic content (total organic carbon < 2.87 wt%, kerogen type II/III) and low thermal maturity (temperature of maximum hydrocarbon generation < 438 °C) of the organic matter indicate that gaseous hydrocarbon production is the result of bacterial metabolism. The dissolved and void gases contain CH_4 as the main hydrocarbon component with small amounts of C_2H_6, and C_3H_8. The isotopic signatures of the dissolved gas ($\delta^{13}C_{CH4}$ < −51.5‰, δD_{CH4} < −206‰) indicate a biogenic origin. On the other hand, the $\delta^{13}C_{CH4}$ of the void gas exceeds that of the dissolved gas, increasing from the southern part ($\delta^{13}C_{CH4}$ < −59.5‰) to the northern part ($\delta^{13}C_{CH4}$ < −22.9‰) of the study area. The presence of ^{13}C-rich CH_4, C_2H_6, and C_3H_8 as well as the $\delta^{13}C_{CH4}$ vs. $\delta^{13}C_{C2H6}$ correlation of the dissolved and void gases indicate a mixed biogenic/ thermogenic origin. This study suggests that the biogenic gas was most likely generated in the early biogenic gas system and it has been mixed with thermogenic gas migrated from the deeper part.

Key words: Pohang Basin, shallow biogenic gas, early-generation system, total organic carbon, hydrocarbon gas

Manuscript received March 2, 2021; Manuscript accepted October 12, 2021

1. INTRODUCTION

Biogenic gas holds great promise as a green energy source, accounting for ~20% of global natural gas reserves (Rice and Claypool, 1981). Among the numerous components of biogenic gas, microbial CH_4 is of particular economic interest due to its relatively low production cost. Commercial biogenic gas fields are distributed worldwide, as exemplified by the gas fields in the Hangzhou Bay, China (Pang et al., 2005; Li and Lin, 2010), the eastern Denver Basin, USA (Rice, 1984), and the southeastern Alberta Basin, Canada (Ridgley et al., 1999).

Shallow biogenic gas is natural gas generated by anaerobic bacteria from organic-rich thermally immature source rocks. Favorable conditions for its generations are (1) anoxic conditions, (2) low levels of electron acceptors (e.g., sulfates and nitrates), (3) low temperature, and (4) abundant organic matter (OM) (Rice, 1993). Compared with conventional petroleum gas systems, shallow biogenic gas systems are characterized by accumulations in geologically younger, moderate temperature (typically below 80 °C), and low pressure reservoirs (Rice, 1993; Shurr and Ridgley, 2002). The most useful properties to distinguish biogenic gas from other gases are the gas composition and isotope characteristics. Biogenic gas consists mainly of methane ($C_1/C_{1+} > 0.98$). In particular, biogenic gas is typically characterized by a lighter carbon isotope ratio of methane (−110 – −50‰) than thermogenic gas generated in conventional systems (−50 – −20‰) (Whiticar, 1999).

Shallow biogenic gas systems can be divided into early- and late-generation systems based on the proximity of the gas generation and accumulation region and the timing of the gas generation (Rice, 1993; Shurr and Ridgley, 2002). Early-generation systems are characterized by gas generation occurring immediately after deposition of the source and reservoir rocks, with the result that the geological time of the carbon-source formation

*Corresponding author:
Jiyoung Choi
Oil and Gas Research Center, Petroleum and Marine Research Division, Korea Institute of Geoscience and Mineral Resources (KIGAM), 124 Gwahak-ro, Yuseong-gu, Daejeon 34132, Republic of Korea
Tel: +82-42-868-3252, Fax.: +82-42-868-3417,
E-mail: jychoi@kigam.re.kr

and biogenic-gas generation is approximately same (Rice and Shurr, 1980; Rice and Claypool, 1981; Rice, 1993; Shurr and Ridgley, 2002). On the other hand, late-generation systems are characterized by the gas generation occurring much later than the deposition of the source and reservoir rocks, as indicated by older carbon sources and relatively new biogenic gas (Rice, 1993; Martini et al., 1996; Martini et al., 1998; Shurr and Ridgley, 2002). Therefore, methanogenic microbes and their habitable environment may have been active in the relatively recent geologic past in late-generation systems, but disappeared early in early-generation systems (Shurr and Ridgley, 2002; Shurr, 2008). Consequently, the differences between the two biogenic systems affect the location of the biogenic gas accumulations. In early-generation systems, biogenic gas is usually accumulated on the margins of the depositional basin, controlled by paleotectonism and deposition variation (Shurr and Ridgley, 2002; Shurr, 2008). On the other hand, in late-generation systems, biogenic gas is accumulated on the margins of structural basins and the accumulation is influenced by modern environmental conditions such as groundwater flow patterns (Shurr and Ridgley, 2002; Shurr, 2008). It is important to understand biogenic gas generation systems to identify prospective areas where gas exploration and development are expected.

In 2017, drilling activities for the 200-m-deep well construction in the Pohang Basin triggered a sudden eruption of underground natural gas that caught fire and continued burning for more than 4 years (Kang et al., 2019). This accident caused a regional investigation of the gas reserve distribution in the Pohang Basin. However, related studies on gas properties and generation mechanisms remain scarce. To bridge this gap, this work aims to shed light on the shallow gas systems of the Pohang Basin by probing hydrocarbon gas characteristics, organic matter quality and content, and source rock maturity. In particular, the compositions and isotopic signatures of the dissolved and void gases are studied to determine their origin and gain valuable insights into the evolution of the shallow gas system in the Pohang Basin.

2. GEOLOGICAL SETTING

The Miocene Pohang Basin, located in the southeastern part of the Korean Peninsula, was formed between the Yangsan and Hupo fault systems, which have experienced right-lateral strike-slip movement since the Late Cretaceous and Early Miocene, respectively (Chough et al., 1990; Hwang et al., 1995; Yoon and Chough, 1995; Sohn and Son, 2004). The basin fill deposit (Yeonil Group) is more than 1 km thick and largely comprises conglomerates, sandstones, and mudstones. Lithostratigraphically, the Yeonil Group can be divided into the Chunbuk Conglomerate, Hakjeon, Heunghae, and Duho formations in ascending order (Kim, 1965; Yoon, 1975; Yun, 1986). Detailed studies on clast composition, lithofacies, facies organization, and paleocurrent patterns in the western part of the basin reveal six fan delta systems, deposited in alluvial fan, braided stream, Gilbert-type top-, fore- and bottom sets, prodelta, slope apron, and basin plain environments (Hwang, 1993; Hwang et al., 1995). The vertical and lateral distribution of facies organizations, unconformities, and abrupt changes in lithofacies revealed four evolution stages. Stage 1 (latest Early Miocene) corresponds to the deposition of shallow marine fan deltas in the western margin of the basin and shallow marine mudstones in the basin center. Stage 2 (early Middle Miocene) involves the rapid subsidence of the basin and the deposition of coarse-grained fan deltas in the western margin and deep marine mudstones in the basin center. Stage 3 (Middle Miocene) corresponds to the progradation of fine-grained fan deltas in the western basin margin and the deposition of hemipelagic mudstones and various sediment gravity flow deposits in the basin center. Stage 4 (Late Miocene) involves the decrease in clastic input and the deposition of thick biogenic mudstones (Hwang et al., 1995; I.G. Hwang et al., unpublished manuscript).

3. MATERIAL AND METHOD

3.1. Wells

In this study, we used core cutting, dissolved gas, and void gas samples from five drilling wells, which were recovered during 2017–2020 in Pohang city for shallow gas research (Fig. 1 and Table 1). Five study wells, PD-01, PD-02, PSG-01, PSG-02, and PSG-03, were collected from northeast to southwest within the Pohang Basin. PD-01 and PD-02 wells were drilled and analyzed in 2017 on the basis of the joint research comprising Korea Gas Cooperation (KOGAS), Korea Institute of Geoscience and Mineral Resources (KIGAM) and Pohang city (Kang et al., 2019). PSG-01, PSG-02 and PSG-03 wells were conducted from 2018 to 2020 based on Research and Development (R&D) project from Korea Institute of Energy Technology Evaluation and Planning (KETEP) and KIGAM. The drilling well thickness was approximately 301.1 m for PD-01, 268.5 m for PD-02, 274.1 m for PSG-01, 360.8 m for PSG-02, 289.7 m for PSG-03.

The sedimentological investigations contain detailed lithological analysis, primary sedimentary structures, identification of facies with their thicknesses as well as facies relationships and contacts between them. Sedimentary rocks are grouped according to their formation process and sedimentary properties.

3.2. Sampling for Rocks and Gases

For organic geochemical analysis of bulk rocks, representative

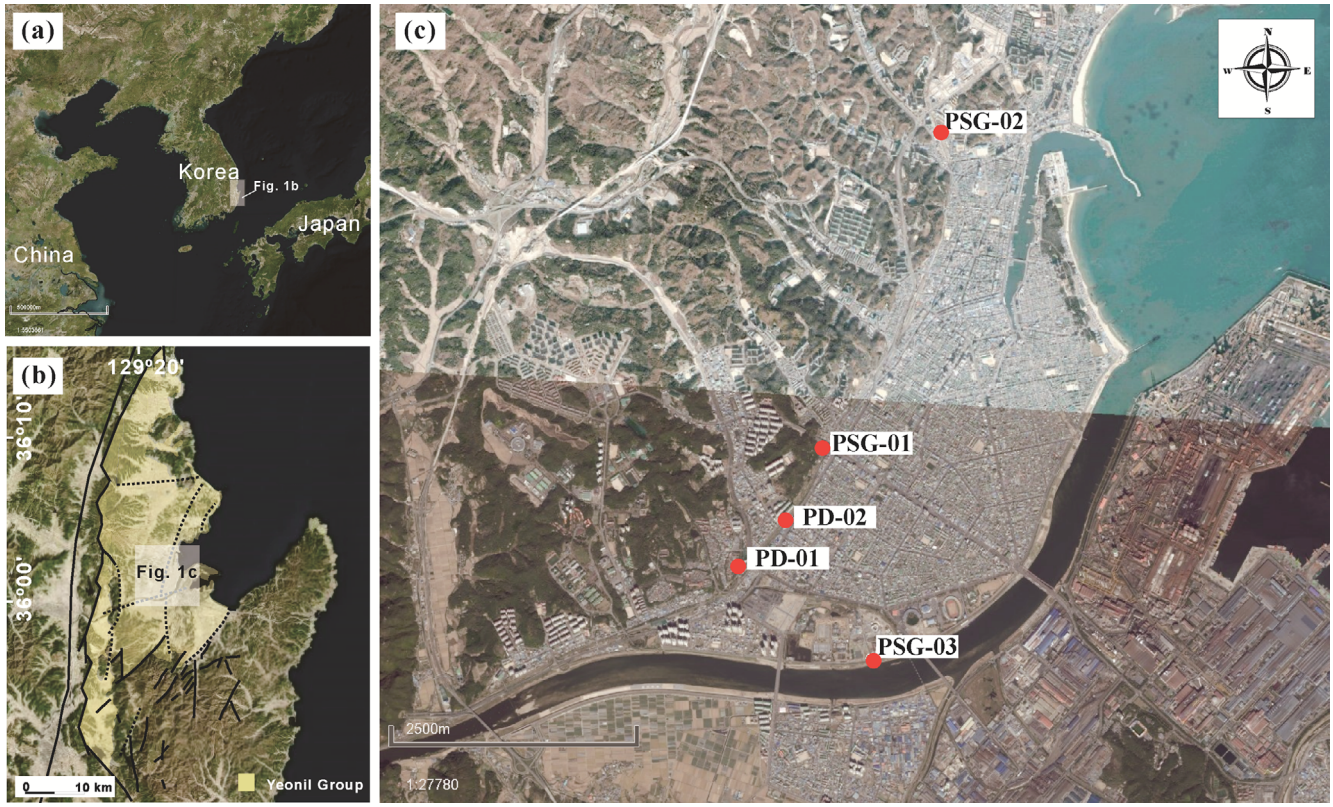

Fig. 1. Location maps showing (a) the Pohang Basin, (b) the Yeonil Group in the Pohang Basin, and (c) wells.

Table 1. Summary of well locations, drilling depth, and sample numbers

Well	Location		Drilling depth (mbgl[(a)])	Number of analyzing sample		
	Latitude	Longitude		Bulk rock	Dissolved gas	Void gas
PD-01	36°00′45.29″N	129°20′25.39″E	301.1	12	17	3
PD-02	36°01′00.10″N	129°20′44.70″E	268.5	12	13	0
PSG-01	36°01′23.69″N	129°20′58.70″E	274.1	9	14	4
PSG-02	36°03′06.99″N	129°20′44.70″E	360.8	10	11	0
PSG-03	36°00′15.00″N	129°21′16.50″E	289.7	12	12	4

[(a)]mbgl: meter below ground level.

cutting samples have been selected in organic-rich parts from hemipelagic and turbidities mud (Table 2). The selected samples were crushed to a particle size of > 100 mesh.

Void gas samples were directly collected from wellhead bypass through blow out preventer (BOP) assembly connected to a wellhead. Dissolved gas samples were obtained from water-based muds (drilling mud) at intervals of 10 m to 20 m that was produced when the wells were recovered. Briefly, drilling mud (3 mL) was extruded into a 21-mL-headspace glass vial that was immediately capped with a rubber septum, sealed with an aluminum crimp cap, heated at 65 °C for 30 min for degassing, and subjected to the dissolved gas sampling (Pimmel and Claypool, 2001). The geochemical data for PD-01 and PD-02 wells were used from materials published by Choi et al. (2019).

3.3. Analysis of Organic Matter Composition

OM analysis was performed using crushed samples (60–70 mg) prepared using a Rock-Eval6 Turbo instrument at KIGAM. For petroleum potential evaluation, the source rocks were heated from 300 to 650 °C in a pyrolysis oven and from 300 to 850 °C in an oxidation oven, and the released hydrocarbons were monitored by a flame ionization detector and assigned to free hydrocarbons (S_1) and kerogen (S_2) (Lafargue et al., 1998). The temperature of maximum hydrocarbon generation (T_{max}) was calculated as the temperature corresponding to the highest intensity of the S_2 peak (Lafargue et al., 1998). The organic carbon content was defined as pyrolysable organic carbon (PC, analyzed in the pyrolysis oven) and residual organic carbon (RC, analyzed in the oxidation oven). Total organic carbon (TOC) was defined as PC + RC. Vinci's

https://doi.org/10.1007/s12303-021-0035-1

Table 2. Results of OM composition and $\delta^{13}C_{org}$ of bulk rocks (data of PD-01 and PD-02 are sourced from Choi et al., 2019)

Well	Depth (mbgl)	Unit	Lithology	S_1 (mgHC/gRock)	S_2 (mgHC/gRock)	T_{max} (°C)	HI (mgHC/gTOC)	OI (mgCO_2/gTOC)	TOC (wt%)	MINC (wt%)	$\delta^{13}C_{org}$ (‰)
PD-01	16.5	III	Hemipelagic	0.08	4.96	422	314	8	1.58	1.04	–21.8
	120.4	II	Hemipelagic	0.13	5.97	425	353	2	1.69	0.3	–22.76
	139.9	II	Hemipelagic	0.18	7.71	427	372	8	2.07	1.64	–21.46
	155.4	II	Hemipelagic	0.19	7.22	426	374	4	1.93	0.76	–21.52
	169.9	II	Hemipelagic	0.19	6.95	427	370	13	1.88	0.97	–21.78
	174.0	II	Turbidite	0.09	3.78	429	250	8	1.51	0.96	–21.75
	195.0	I	Hemipelagic	0.18	6.8	430	400	2	1.7	0.52	–21.02
	205.4	I	Turbidite	0.16	6.22	430	391	5	1.59	1.27	–21.29
	219.7	I	Hemipelagic	0.21	8.18	429	437	2	1.87	0.38	–21.47
	245.2	I	Hemipelagic	0.22	6.48	429	368	2	1.76	0.5	–22.08
	270.8	I	Hemipelagic	0.23	8.06	426	436	3	1.85	0.22	–21.34
	295.4	I	Hemipelagic	0.23	8.29	426	384	5	2.16	0.18	–22.93
PD-02	10.1	III	Turbidite	0.08	2.93	420	266	25	1.1	0.69	–22.98
	45.0	III	Hemipelagic	0.09	5.24	424	282	19	1.86	1.05	–22.92
	65.0	II	Hemipelagic	0.17	7.54	419	366	15	2.06	0.54	–22.97
	82.0	II	Hemipelagic	0.26	9.67	419	372	42	2.6	1.92	–21.43
	116.2	II	Hemipelagic	0.15	6.51	426	344	8	1.89	0.81	–23.56
	125.1	II	Turbidite	0.25	10.81	427	378	13	2.86	1.53	–22.25
	150.2	II	Hemipelagic	0.24	11.29	423	393	2	2.87	0.25	–21.96
	162.0	II	Hemipelagic	0.22	9.11	423	389	5	2.34	0.75	–21.64
	193.8	II	Turbidite	0.08	3.39	428	235	10	1.44	0.99	–22.77
	214.9	I	Hemipelagic	0.15	6.17	428	388	6	1.59	0.59	–21.87
	244.9	I	Turbidite	0.11	4.37	426	331	7	1.32	0.63	–22.84
	268.0	I	Turbidite	0.17	7.44	423	443	2	1.68	0.18	–22.49
PSG-01	39	III	Hemipelagic	0.19	8.35	426	351	18	2.38	0.56	–22.29
	72	III	Turbidite	0.13	4.29	426	262	22	1.64	0.51	–22.59
	99	III	Hemipelagic	0.17	5.76	428	305	20	1.89	0.72	–22.13
	138	II	Turbidite	0.2	5.74	426	310	9	1.85	0.37	–22.99
	165	II	Hemipelagic	0.3	9.83	424	381	22	2.58	0.93	–22.36
	199	II	Turbidite	0.32	8.93	425	408	7	2.19	0.42	–22.04
	232	II	Hemipelagic	0.2	6.01	424	308	32	1.95	2.82	–21.34
	247	II	Hemipelagic	0.35	10.73	428	467	6	2.3	0.67	–22.47
	262	II	Turbidite	0.12	3.95	431	253	13	1.56	0.88	–21.23
PSG-02	35.9	III	Hemipelagic	0.34	10.32	426	420	5	2.46	0.62	–22.11
	71.8	III	Turbidite	0.27	7.99	426	373	4	2.14	0.78	–21.76
	131	III	Hemipelagic	0.32	7.51	425	397	12	1.89	0.45	–21.77
	183.8	III	Hemipelagic	0.32	6.78	431	348	12	1.95	0.88	–21.97
	213.8	III	Turbidite	0.31	5.6	433	344	8	1.63	0.31	–22.16
	244.5	III	Hemipelagic	0.48	6.66	434	335	14	1.99	0.59	–22.03
	292.5	II	Turbidite	0.51	5.35	436	315	6	1.7	0.39	–23.38
	319.8	II	Hemipelagic	0.99	10.84	438	425	5	2.55	0.56	–22.11
	351.2	II	Turbidite	0.34	4.49	438	314	6	1.43	0.45	–21.99
	360.8	I	Hemipelagic	0.51	5.47	438	362	9	1.51	0.73	–21.52
PSG-03	55.4	III	Hemipelagic	0.09	4.03	420	265	26	1.52	0.45	–
	78.5	III	Turbidite	0.1	4.7	419	305	25	1.54	0.27	–
	86.4	III	Hemipelagic	0.1	5.93	421	341	20	1.74	0.37	–
	111.1	III	Turbidite	0.07	3.39	425	255	42	1.33	0.5	–
	138.9	II	Hemipelagic	0.17	4.99	421	333	69	1.5	0.56	–
	160.1	II	Turbidite	0.11	4.57	420	257	30	1.78	0.54	–
	197.1	II	Hemipelagic	0.1	4.88	421	301	48	1.62	2.41	–
	208.4	II	Turbidite	0.17	7.06	419	358	23	1.97	0.31	–
	230.3	II	Hemipelagic	0.13	5.21	424	306	21	1.7	0.46	–
	254.6	II	Turbidite	0.17	3.87	422	256	36	1.51	0.26	–
	286.7	I	Hemipelagic	0.17	5.13	425	344	38	1.49	0.92	–
	289.7	I	Turbidite	0.18	4.9	426	325	38	1.51	0.32	–

IFP160,000 was used as a standard, and the reproducibilities of the S_1, S_2, and TOC analyses were found to be less than 0.07, 0.25, and 0.07%, respectively.

For the ^{13}C content analysis, powdered samples were pretreated with 3 N hydrochloric acid to remove carbonate minerals and then analyzed using a continuous-flow stable isotope ratio mass spectrometer (Isoprime-EA, Micromass, UK) linked to a CN analyzer (NA Series 2, CE Instruments, Italy) at the Seoul National University National Instrumentation Center for Environmental Management. Isotope contents are presented as ‰ deviations from Peedee Belemnite (PDB) values, and the analysis reproducibility was determined as ±0.1‰.

3.4. Analysis of Hydrocarbon Gases

Gas compositions and concentrations were measured using an Agilent 7890A gas chromatograph equipped with a 50-m fused silica column (0.32 mm × 0.5 μm) and a flame ionization detector. The column temperature was maintained at 35 °C for 5 min and then increased to 195 °C at 20 °C/min. The reproducibility was less than 5%, as determined by repeated standard analyses.

The contents of stable carbon (^{13}C) and hydrogen (D) isotopes ($\delta^{13}C$ and δD, reported in permil (‰) relative to V-PDB and V-SMOW, respectively) in CH_4 and the $\delta^{13}C$ of C_2H_6 and CO_2 in the gas samples were analyzed using a compound-specific isotope ratio-monitoring gas chromatograph/mass spectrometer (Isotech Laboratories Inc., Champaign, IL, USA). The reproducibilities were determined as 0.1‰ for $\delta^{13}C$ and 2‰ for δD.

4. RESULTS

4.1. Lithological Study

The cored interval drilled for this study (PD-01, PD-02, PSG-01, PSG-02, and PSG-03 wells) belongs to Stages 3 and 4 successions of the Pohang Basin deposited in slope apron and basin plain environments. Most of the sampled mudstones were deposited by hemipelagic settling and low-density turbidity current, containing various fossils such as wood and leaf fragments, sponge spicules, and foraminifers. This study divided the sedimentary succession of the study area into four units based on the sedimentary core descriptions of wells PD-01, PD-02, PSG-01, PSG-02 and PSG-03. These units can be correlated to the Stage 3 and 4 deposits of Yeonil Group in Pohang Basin, deposited by hemipelagic settling and sediment gravity flows in base of slope and basin plain environment (Stage 3) and slow settling of biogenic mudstone in basin plain environments (Stage 4) (Hwang et al., 1995). Unit-I occupies the lower most part above the core and is dominated by hemipelagic mudstone, with thin layers of sandstone, commonly less than 10 centimeters in thickness. Unit-II overlying the Unit-I is bounded by thick turbidite sandstone more than 6 m in thickness at the lower part. The thick turbidite layer occurs in all wells that analyzed for this study. Unit-II is characterized by thick hemipelagic mudstone intercalated with relatively thick turbidite sandstone and mudstone layers. Comparing to Unit-I, frequency and thickness of these sandy or silty layers increased dramatically in Unit-II. Unit-III overlain by Unit-II occupies top of Middle Miocene succession. The lithology of Unit-III is similar to that of Unit-II. The basal surface of Unit-III is defined as widely distributed dacitic ash layer. SHRIMP age dating of zircon suggests that the volcanic eruption occurred approximately 14.7 ± 0.2 Ma (I.G. Hwang et al., unpublished manuscript). Unit-IV is represented by light yellowish grey mudstone, deposited by slow settling of biogenic grains and clastic mudstone in basin plain environment. This unit is finally overlain by Quaternary alluvium with erosional boundary.

4.2. Organic Matter Characteristics

TOC ranged from 1.10 to 2.87 wt% (average = 1.85 wt%, n = 55) and was the highest at PSG-01 (average = 2.04 wt%, n = 9) and the lowest at PSG-03 (average = 1.6 wt%, n = 12).

S_1 ranged from 0.07 to 0.99 mgHC/gRock (average = 0.22 mg_{HC}/g_{rock}, n = 55) and was the highest at PSG-02 (average = 0.44 mgHC/gRock) and the lowest at PSG-03 (average = 0.13 mgHC/gRock).

S_2 ranged from 2.93 to 11.29 mgHC/gRock (average = 6.52 mgHC/gRock, n = 55) and was the highest at PSG-02 (average = 7.1 mgHC/gRock) and the lowest at PSG-03 (average = 4.89 mgHC/gRock). For any given sample, TOC, S_1, and S_2 were the highest in Unit II (Table 2 and Fig. 2).

Maturation of OM can be estimated by the range of T_{max}; T_{max} < 435 °C indicates an immature zone, T_{max} = 435–465 °C a mature zone, and T_{max} > 465 °C an overmature zone, respectively (Espitalié et al., 1985). T_{max} (419–438 °C; average = 426 °C, n = 55) was lower than 435 °C for PD-01, PD-02, PSG-01, and PSG-03, indicating immature OM, whereas values above 435 °C were observed for PSG-02, indicating mature OM.

The $\delta^{13}C_{org}$ of PD-01, PD-02, PSG-01, and PSG-02 ranged from –23.6‰ to –21.0‰ (average = –22.1‰, n = 43) and was almost constant with depth, indicating independence with Units I–III (Table 2).

4.3. Gas Composition and Isotope Signatures

Table 3 lists the compositions and isotope signatures of the dissolved gas samples, revealing that they mostly contained CH_4

https://doi.org/10.1007/s12303-021-0035-1

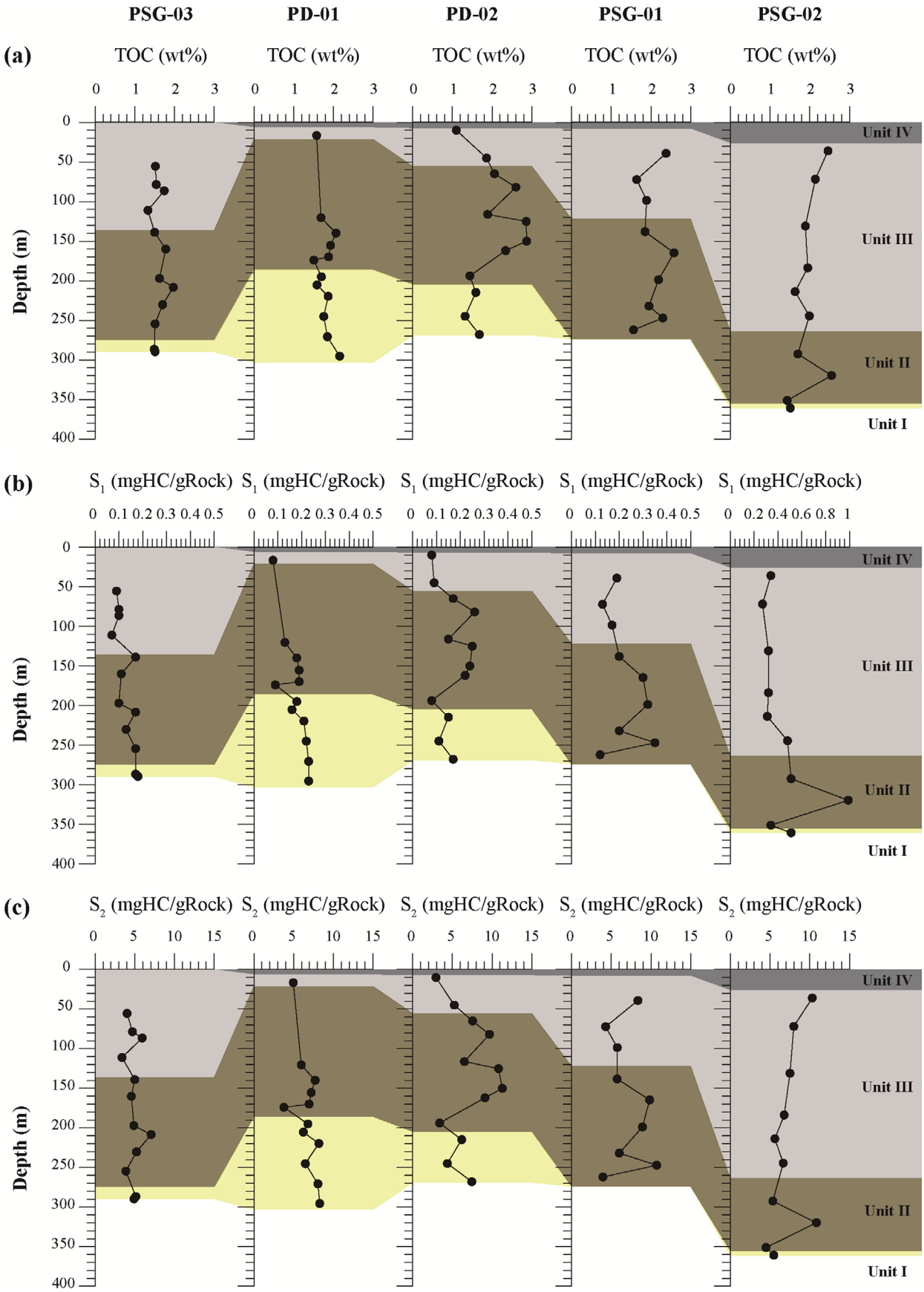

Fig. 2. Vertical variation of (a) TOC, (b) S_1, and (c) S_2 of bulk rocks in five wells.

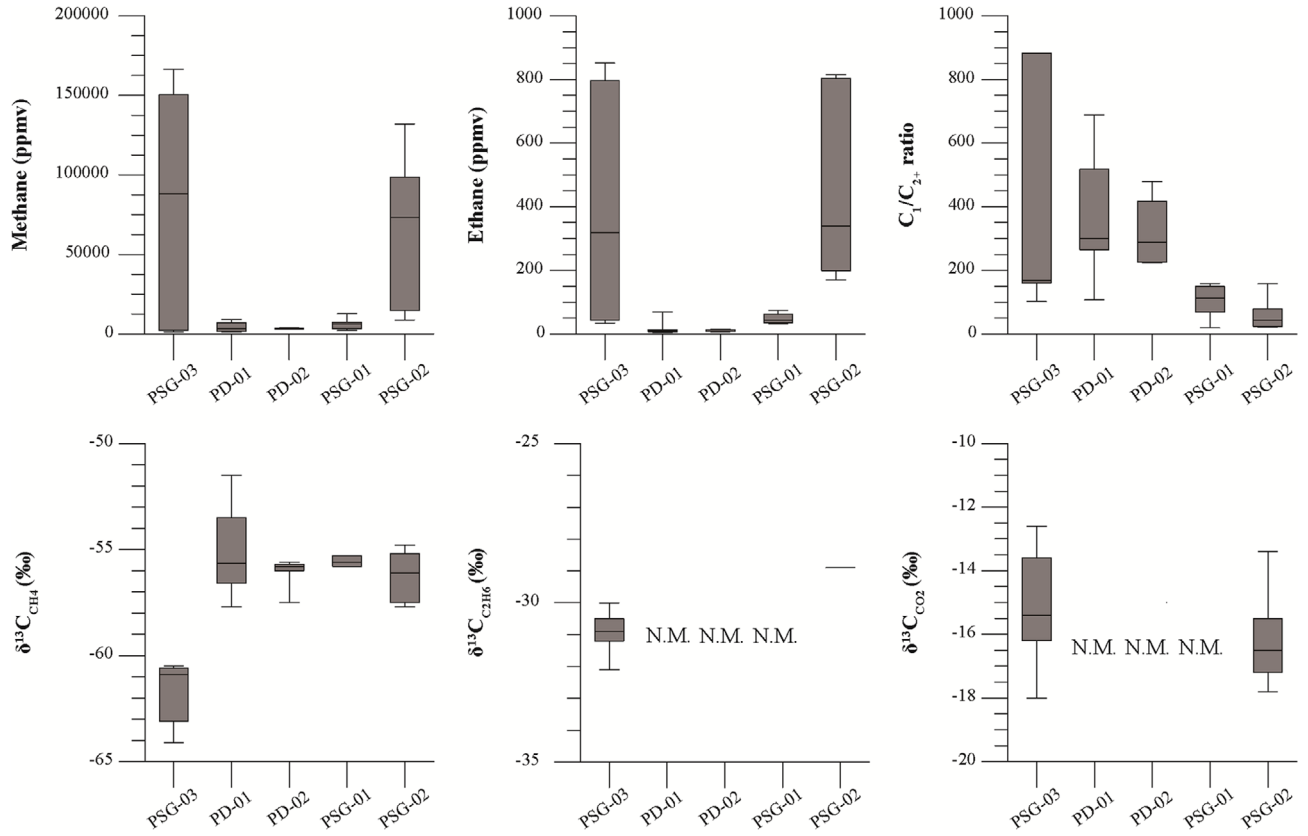

Fig. 3. Composition and isotopic signatures of the dissolved gas.

(> 94 vol%) as well as C_2H_6 (0.04 vol%) and minor amounts of C_{3+} hydrocarbons. The CH_4 concentrations were the highest for PSG-03 (average = 70,560 ppmv, n = 12) and the lowest for PD-01 (average = 6,925 ppmv, n = 17), while the C_2H_6 concentrations were the highest for PSG-02 (average = 496 ppmv, n = 11) and the lowest for PD-02 (average = 13 ppmv, n = 13). The C_1/C_{2+} ratios of the dissolved gas equaled 421, 677, 128, 56, and 210 for PD-01, PD-02, PSG-01, PSG-02, and PSG-03, respectively. The minimum values of $\delta^{13}C_{CH4}$ in the dissolved gas samples occured in PSG-03 (Fig. 3).

Table 4 lists the compositions and isotope signatures of the void gas samples, revealing that they mostly contained CH_4 (> 99 vol%) as well as C_2H_6 (0.02 vol%) and minor amounts of C_{3+} hydrocarbons. The C_1/C_{2+} ratios of the void gas generally exceeded 2,640 for PD-01, 1,824 for PSG-01, and 192 for PSG-03, respectively. For $\delta^{13}C_{CH4,}$ the minimum value was observed in PSG-03 and the maximum value in PSG-01 (Fig. 4).

5. DISCUSSION

5.1. Organic Matter Characteristics

A sufficient amount of OM (TOC > 0.5 wt%) is necessary for biogenic (i.e., microbial) gas generation (Rice, 1993). The TOC values (1.1–2.87 wt%) at five wells are sufficient for biogenic gas generation (Fig. 5). The S_2 values in this study range from 2.93 to 11.29 mgHC/gRock, indicating a fair to very good potential for hydrocarbon gas generation (Fig. 5; Peters and Cassa, 1994).

The HI values ranged from 235–467 mg/g at five wells, indicating the potential for gases to produce predominantly oil-gas mixtures (Kerogen type II and III) (Waples, 1985). The modified van Krevelen diagram shows that all wells most likely contain Type II/III marine OM (Fig. 6). In addition, the $\delta^{13}C_{org}$ ranging from –23.56‰ to –21.02‰ also supports that the organic matter in the study area is predominantly particulate OM produced mainly by marine phytoplankton (Lamb et al., 2006). Our results indicate the dominant influence of particulate organics synthesized by marine phytoplankton, supporting the dominance of Type II/III OM within the cored interval.

Thermal maturity is another important factor for biogenic gas generation. T_{max} measured from all samples except for PSG-02 shows that OM is thermally immature (Fig. 7). In the case of PSG-02, T_{max} equaled 425–434 °C in Unit III, 436–438 °C in Unit II, and 438 °C in Unit I (Fig. 7), indicating maturity from Unit II onward. Generally, T_{max} is used to define the size of the burial,

https://doi.org/10.1007/s12303-021-0035-1

Table 3. Molecular and isotopic signatures of the dissolved gas (data for PD-01 and PD-02 are taken from Choi et al., 2019)

Well	No.	Concentration			C_1/C_{2+} ratio	Relative ratio			Stable isotope values			
		C_1 (ppmv)	C_2 (ppmv)	C_3 (ppmv)		C_1 (%)	C_2 (%)	C_3 (%)	$\delta^{13}C_1$ (‰)	$\delta^{13}C_2$ (‰)	δD_{C1} (‰)	$\delta^{13}CO_2$ (‰)
PD-01	1	3,349	14	n.d.	238	99.58	0.42	0.00	−57.7	–	–	–
PD-01	2	1,575	6	n.d.	265	99.62	0.38	0.00	–	–	–	–
PD-01	3	4,728	13	n.d.	364	99.73	0.27	0.00	-56.0	–	–	–
PD-01	4	7,071	14	n.d.	517	99.81	0.19	0.00	–	–	–	–
PD-01	5	38,614	35	n.d.	1,116	99.91	0.09	0.00	−56.6	–	−220	–
PD-01	6	9,180	13	n.d.	688	99.85	0.15	0.00	–	–	–	–
PD-01	7	20,852	16	n.d.	1,295	99.92	0.08	0.00	−51.5	–	−214	-
PD-01	8	3,977	9	n.d.	455	99.78	0.22	0.00	–	–	–	–
PD-01	9	1,976	6	n.d.	315	99.68	0.32	0.00	–	–	–	–
PD-01	10	3,159	10	n.d.	312	99.68	0.32	0.00	–	–	–	–
PD-01	11	3,992	20	n.d.	200	99.50	0.50	0.00	−53.5	–	−219	–
PD-01	12	1,253	7	n.d.	184	99.46	0.54	0.00	–	–	–	–
PD-01	13	2,186	9	n.d.	247	99.60	0.40	0.00	–	–	–	–
PD-01	14	1,255	4	n.d.	287	99.65	0.35	0.00	–	–	–	–
PD-01	15	960	3	n.d.	275	99.64	0.36	0.00	–	–	–	–
PD-01	16	7,456	69	n.d.	107	99.08	0.92	0.00	–	–	–	–
PD-01	17	6,149	21	n.d.	290	99.66	0.34	0.00	−55.3	–	−220	-
Average		6,925	16	–	421	99.66	0.34	–	−55.1	–	–	–
PD-02	1	1,021	4	n.d.	273	99.63	0.37	0.00	–	–	–	–
PD-02	2	3,106	14	n.d.	226	99.56	0.44	0.00	–	–	–	–
PD-02	3	4,255	30	n.d.	142	99.30	0.70	0.00	–	–	–	–
PD-02	4	4,117	14	n.d.	305	99.67	0.33	0.00	−55.8	–	–	–
PD-02	5	2,886	10	n.d.	277	99.64	0.36	0.00	–	–	–	–
PD-02	6	3,698	8	n.d.	479	99.79	0.21	0.00	–	–	–	–
PD-02	7	52,652	24	n.d.	2,219	99.95	0.05	0.00	−55.7	–	–	–
PD-02	8	3,420	15	n.d.	224	99.56	0.44	0.00	–	–	–	–
PD-02	9	7,418	11	n.d.	661	99.85	0.15	0.00	−56.0	–	–	–
PD-02	10	2,965	7	n.d.	416	99.76	0.24	0.00	–	–	–	–
PD-02	11	20,544	9	n.d.	2,344	99.96	0.04	0.00	−55.6	–	–	–
PD-02	12	3,800	14	n.d.	273	99.63	0.37	0.00	–	–	–	–
PD-02	13	5,736	6	n.d.	968	99.90	0.10	0.00	−57.5	–	–	–
Average		8,894	13	–	677	99.71	0.29	–	−56.1	-	–	–
PSG-01	1	567	13	22	16	94.18	2.15	3.67	–	–	–	–
PSG-01	2	2,168	53	57	20	95.15	2.33	2.52	–	–	–	–
PSG-01	3	4,289	63	61	35	97.19	1.44	1.38	−55.8	–	–	–
PSG-01	4	5,653	42	8	112	99.12	0.73	0.15	–	–	–	−20.7
PSG-01	5	5,390	32	22	101	99.02	0.58	0.40	–	–	–	–
PSG-01	6	12,643	74	11	149	99.33	0.58	0.08	–	–	–	–
PSG-01	7	8,352	30	12	201	99.50	0.36	0.14	–	–	–	–
PSG-01	8	3,171	34	12	69	98.56	1.07	0.36	–	–	–	–
PSG-01	9	7,327	51	9	121	99.18	0.69	0.13	–	–	–	–
PSG-01	10	7,378	62	5	111	99.11	0.83	0.06	–	–	–	–
PSG-01	11	5,439	52	19	77	98.71	0.94	0.35	–	–	–	–
PSG-01	12	6,260	43	13	112	99.12	0.68	0.20	–	–	–	–
PSG-01	13	24,978	38	11	506	99.80	0.15	0.04	−55.6	–	–	–
PSG-01	14	6,872	33	11	159	99.38	0.47	0.15	−55.3	–	–	–
Average		7,178	44	19	128	98.38	0.93	0.69	−55.6	–	–	–

Table 3. (contunued)

Well	No.	Concentration			C_1/C_{2+} ratio	Relative ratio			Stable isotope values			
		C_1 (ppmv)	C_2 (ppmv)	C_3 (ppmv)		C_1 (%)	C_2 (%)	C_3 (%)	$\delta^{13}C_1$ (‰)	$\delta^{13}C_2$ (‰)	δD_{C1} (‰)	$\delta^{13}CO_2$ (‰)
PSG-02	1	4,824	114	173	17	94.38	2.23	3.39	−55.6	–	–	−13.4
PSG-02	2	8,838	170	203	24	95.95	1.85	2.20	−57.4	–	−224	−16.2
PSG-02	3	77,380	654	251	85	98.84	0.84	0.32	−57.5	–	−226	−19
PSG-02	4	98,508	816	1,489	43	97.71	0.81	1.48	−56.8	–	−227	−15.5
PSG-02	5	22,797	436	1,114	15	93.63	1.79	4.58	−54.8	–	−223	−15.8
PSG-02	6	73,083	340	123	158	99.37	0.46	0.17	−57.7	–	−225	−17.2
PSG-02	7	74,048	442	289	101	99.02	0.59	0.39	−55.2	–	−217	−17.8
PSG-02	8	14,649	200	500	21	95.44	1.30	3.26	−54.8	–	−213	−16.5
PSG-02	9	20,400	338	924	16	94.18	1.56	4.26	−55.8	–	−215	−16.8
PSG-02	10	132,004	803	875	79	98.74	0.60	0.65	−56.1	–	−218	−16.6
PSG-02	11	139,548	1,146	1,350	56	98.24	0.81	0.95	−59.2	−28.9	−222	–
Average		60,553	496	663	56	96.87	1.17	1.97	−56.4	−28.9	−221	−16.5
PSG-03	1	706	2	2	n.d.	99.39	0.26	0.35	–	–	–	–
PSG-03	2	2,257	44	54	n.d.	95.87	1.86	2.28	−62.4	–	–	−15.9
PSG-03	3	3,836	37	7	n.d.	98.89	0.94	0.17	−64.1	–	–	−15.4
PSG-03	4	1,461	34	36	n.d.	95.45	2.22	2.34	−63.1	–	–	−15.2
PSG-03	5	24,243	213	51	92	98.92	0.87	0.21	−64.2	–	−214	−18
PSG-03	6	64,529	524	108	102	99.03	0.80	0.17	−61.7	−30.6	−209	−13.6
PSG-03	7	122,328	687	49	166	99.40	0.56	0.04	−59.8	−30	−215	−12.6
PSG-03	8	150,404	852	85	160	99.38	0.56	0.06	−60.9	−30.5	−212	–
PSG-03	9	92,876	459	44	185	99.46	0.49	0.05	−60.9	−31.2	−209	−17.9
PSG-03	10	166,294	796	140	178	99.44	0.48	0.08	−60.5	−32.1	−206	−12.6
PSG-03	11	106,218	212	19	460	99.78	0.20	0.02	−60.6	−31.2	−212	−16.2
PSG-03	12	111,574	114	12	883	99.89	0.10	0.01	−60.7	–	−214	–
Average		70,560	331	51	278	98.74	0.78	0.48	−61.7	−30.9	−211	−15.3

because it increases consistently with burial depth (Guidish et al., 1985). In this study, among the T_{max} values measured at the same depth (200 m) in each of the wells, T_{max} of PSG-02 is approximately 10 °C higher, indicating that the maximum burial depth of PSG-02 was deeper than that of the other wells. This higher thermal maturity of the specimens sampled in the northern part of the basin, resulted from greater burial depths.

5.2. Origin of Hydrocarbon Gas

In the dissolved gas samples, CH_4 and C_2H_6 account for > 94 vol% and < 2 vol% of hydrocarbons, respectively, whereas in the void gas samples, they are equal to 99 vol% and 0.45 vol%, respectively (Tables 3 and 4). In both cases, abundant of CH_4 and traces of C_2H_6 hydrocarbons indicate the biological origin of the hydrocarbon gas. The C_1/C_{2+} ratio of the dissolved gas gradually decreased toward the northern part of the basin and was less than 100 for PSG-02 (Fig. 3). The results of the gas composition analysis indicate differences in the characteristics of the hydrocarbon gases within the basin.

The ^{13}C content of CH_4 ($\delta^{13}C_{CH4}$) can be used to determine whether a gas is generated by biogenic or thermogenic processes (Whiticar, 1999). The $\delta^{13}C$ of the dissolved CH_4 ranges from −59‰ to −52‰ for PD-01, PD-02, PSG-01, and PSG-02, while a value of less than −60‰ is observed for PSG-03 (Fig. 3). Although the $\delta^{13}C_{CH4}$ values of the dissolved gas are location-dependent, they mostly belonged to the range expected for biogenic gas, which is consistent with the thermal evolution (T_{max} < 438 °C) in the study area. The predominant biogenic CH_4 generation pathways, namely CO_2 reduction and acetate fermentation, can be distinguished based on δD_{CH4} values (Whiticar et al., 1986), which range from −400‰ to −250‰ for acetate fermentation and from −250‰ to −145‰ for CO_2 reduction. Herein, δD_{CH4} values ranging from −227‰ to −206‰ (average = −217‰) and from −219‰ to −189‰ (average = −207‰) are observed for the dissolved and void gases, respectively, indicating that CH_4 in the Pohang Basin was primarily generated via microbial CO_2 reduction. However, the $\delta^{13}C_{CH4}$ of the void gas strongly increases toward the north of the basin, corresponding to −61‰ for PSG-03, −45‰ for PD-01, and −28‰ for PSG-01 (Fig. 4). The values of PD-01 and PSG-

https://doi.org/10.1007/s12303-021-0035-1

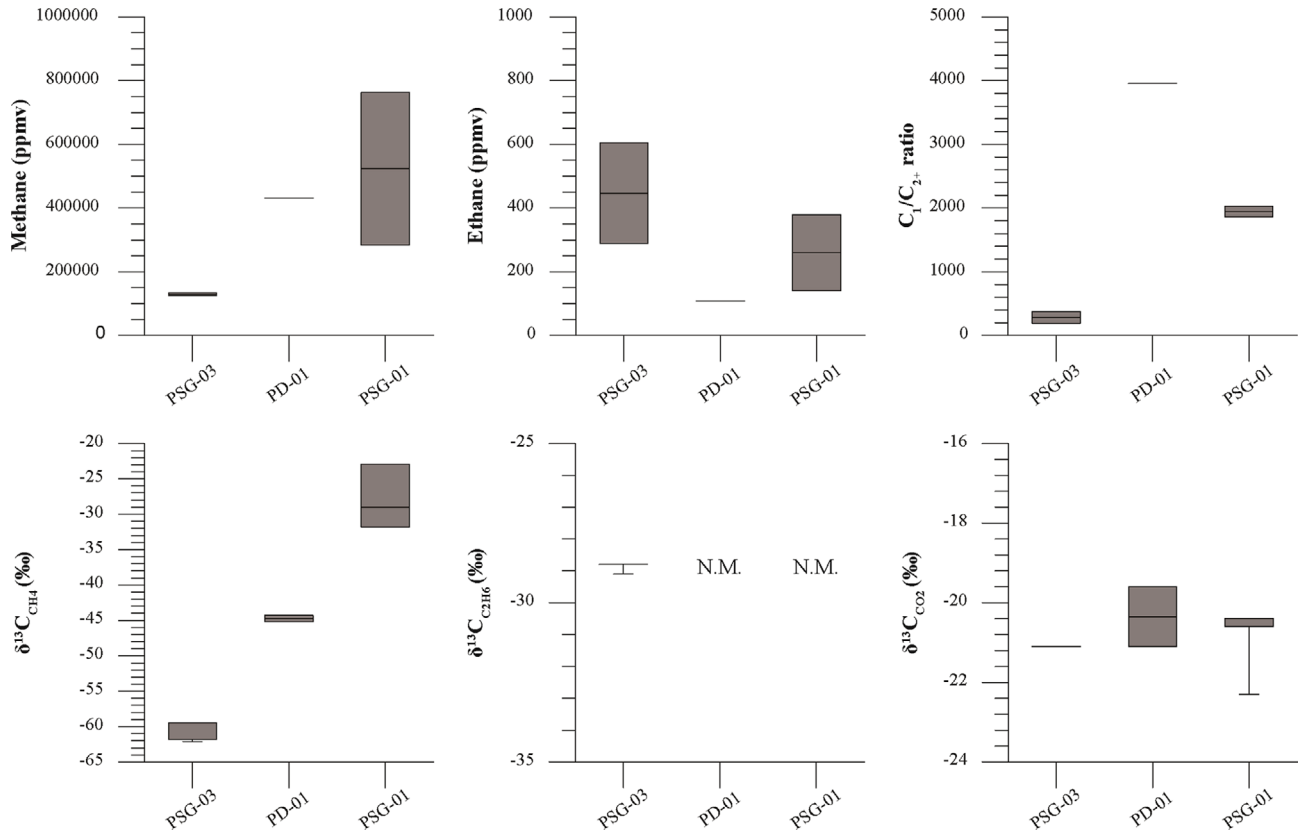

Fig. 4. Composition and isotopic signatures of the void gas.

Table 4. Molecular and isotopic signatures of the void gas (data for PD-01 are taken from Choi et al., 2019)

Well	No.	Concentration			C_1/C_{2+} ratio	Relative ratio			Stable isotope values			
		C_1 (ppmv)	C_2 (ppmv)	C_3 (ppmv)		C_1 (%)	C_2 (%)	C_3 (%)	$\delta^{13}C_1$ (‰)	$\delta^{13}C_2$ (‰)	δDC_1 (‰)	$\delta^{13}CO_2$ (‰)
PD-01	1	559,561	133	n.d.	4,204	99.98	0.02	0.00	−44.3	–	−205	−21.1
PD-01	2	430,532	109	n.d.	3,960	99.97	0.03	0.00	–	–	–	–
PD-01	3	311,456	118	n.d.	2,640	99.96	0.04	0.00	−45.2	–	−210	−19.6
Average		433,850	120	–	3,601	99.97	0.03	–	−44.8	-	–	−20.4
PSG-01	1	684,701	346	29	1,824	99.95	0.05	0.00	−22.9	–	−193	−20.4
PSG-01	2	284,300	140	n.d.	2,031	99.95	0.05	0.00	−31.8	–	−189	−22.3
PSG-01	3	237,700	117	n.d.	2,032	99.95	0.05	0.00	−29.0	–	−192	−20.6
PSG-01	4	762,825	379	31	1,862	99.95	0.05	0.00	–	–	–	–
Average		492,382	246	30	1,937	99.95	0.05	0.00	−27.9	–	–	−21.1
PSG-03	1	133,552	594	91	195	99.49	0.44	0.07	−62.1	−29.1	−219	–
PSG-03	2	133,963	605	94	192	99.48	0.45	0.07	−61.8	−28.8	−218	–
PSG-03	3	130,177	573	88	197	99.49	0.44	0.07	−61.8	−28.8	−218	–
PSG-03	4	125,248	288	45	376	99.73	0.23	0.04	−59.5	−28.8	−215	−21.1
Average		130,735	515	79	240	99.55	0.39	0.06	−61.3	−28.9	−218	−21.1

01 are close to those expected for thermogenic gas, and those of the dissolved and void gases exhibits significant variations (~0.4‰ for PSG-03, 10‰ for PD-01, and 28‰ for PSG-01), which complicates the unambiguous determination of the origin of hydrocarbon gases in the study area. Nevertheless, in the C–D diagram of the dissolved gas, the carbon and hydrogen isotope signatures of CH_4 from all wells are located in the mixed region (Fig. 8). Biogenic CH_4, generated from organic-rich shale at relatively low temperatures and burial depths (T_{max} < 435 °C), is similar to biogenic gases formed shortly after burial in marine

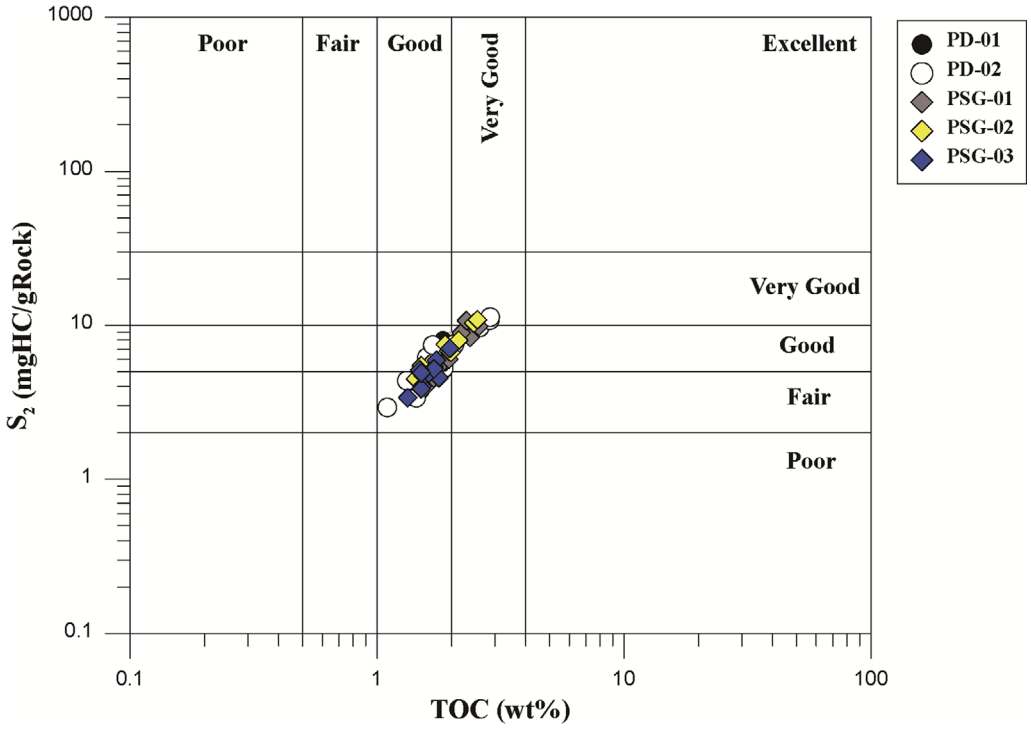

Fig. 5. Cross-plot of TOC and S_2 for different wells.

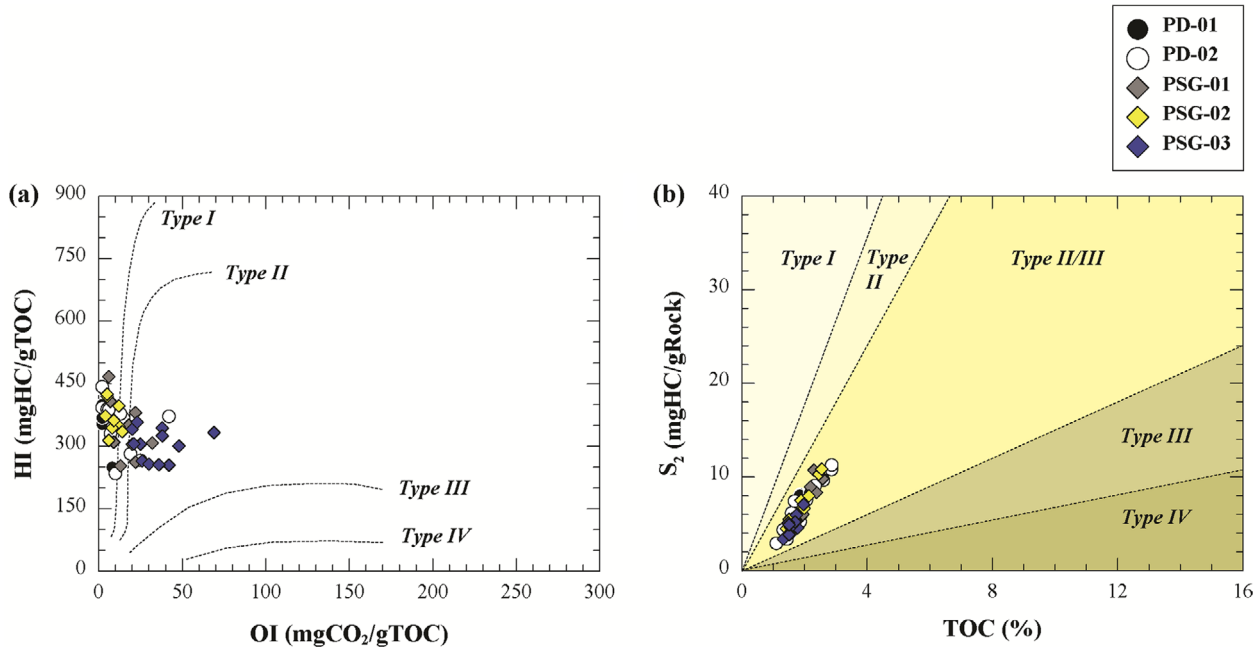

Fig. 6. (a) HI vs. OI and (b) S_2 vs. TOC plots for different wells.

sediments (Claypool and Kaplan, 1974; Rice and Claypool, 1981; Rice, 1993). When the isotopic signatures of hydrocarbon gas obtained in the Pohang Basin are compared with those observed for the adjacent Ulleung Basin, East Sea (Fig. 9), the $\delta^{13}C$ and δD contents of CH_4 and C_2H_6 from the Pohang Basin are found to exceed those of the recently formed CH_4 (–68.5‰) and C_2H_6 (–47.1‰) in the East Sea marine sediments. This demonstration of biogenic origin is important because other carbon isotope criteria for biogenic CH_4 (e.g., $\delta^{13}C_{CH4} < -60‰$) are not clearly met by the Pohang gas (Fig. 9). The pints off result from the relatively high $\delta^{13}C_{CH4}$ in the Pohang Basin.

https://doi.org/10.1007/s12303-021-0035-1

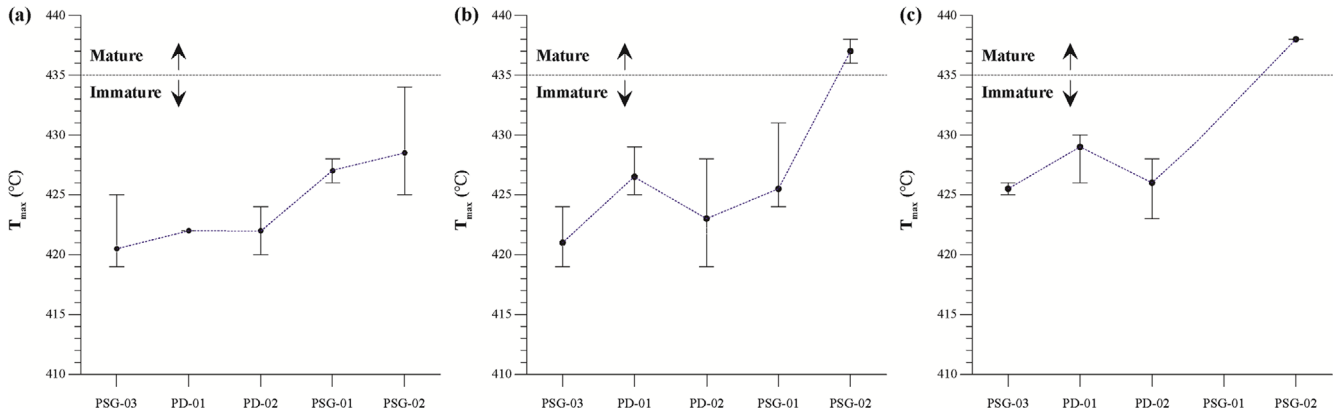

Fig. 7. Thermal maturity variation in (a) Unit III, (b) Unit II, and (c) Unit I.

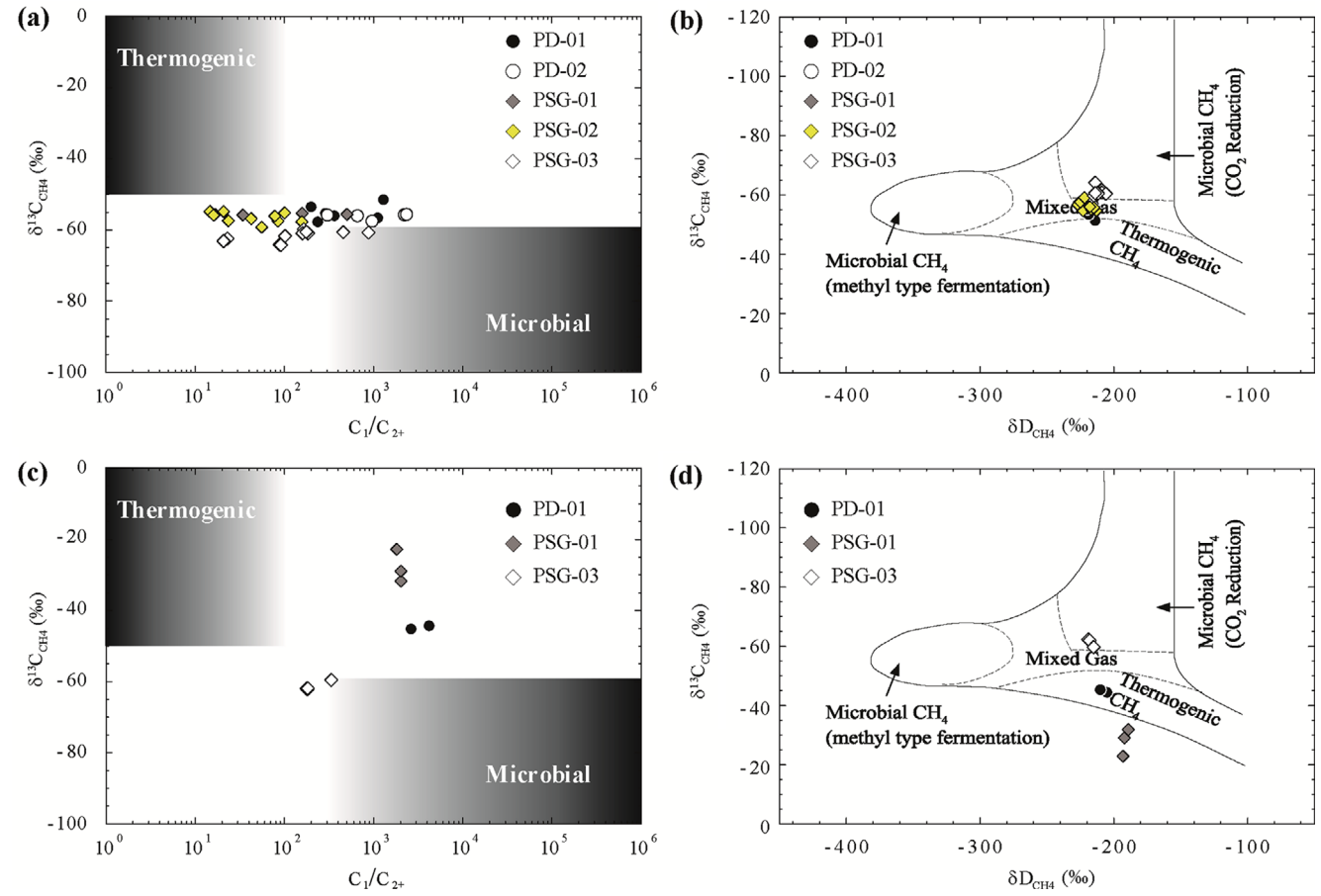

Fig. 8. Origin of the dissolved gas determined using (a) the relationship between the C_1/C_{2+} ratios and $\delta^{13}C_{CH4}$ values of the dissolved gas (modified from Bernard et al., 1978), (b) the $\delta^{13}C_{CH4}$-δD_{CH4} correlation of the dissolved gas (adapted from Whiticar, 1999), (c) the origin of the void gas determined using the relationship between the C_1/C_{2+} ratios and $\delta^{13}C_{CH4}$ values of the void gas (modified from Bernard et al., 1978), and (d) the $\delta^{13}C_{CH4}$-δD_{CH4} correlation of the void gas (adapted from Whiticar, 1999).

5.3. Factors Influencing Heavy Carbon Stable Isotopes of Methane

The $\delta^{13}C_{CH4}$ values measured in this study generally exceed those expected for biogenic gas, which highlights the importance of several possible factors such as microbial oxidation at shallow depth, secondary biogenic gas, and the effects of thermogenic gas. These factors are discussed below for understanding the hydrocarbon gas system of the Pohang Basin.

The isotopic signature of biogenic CH_4 can be changed through

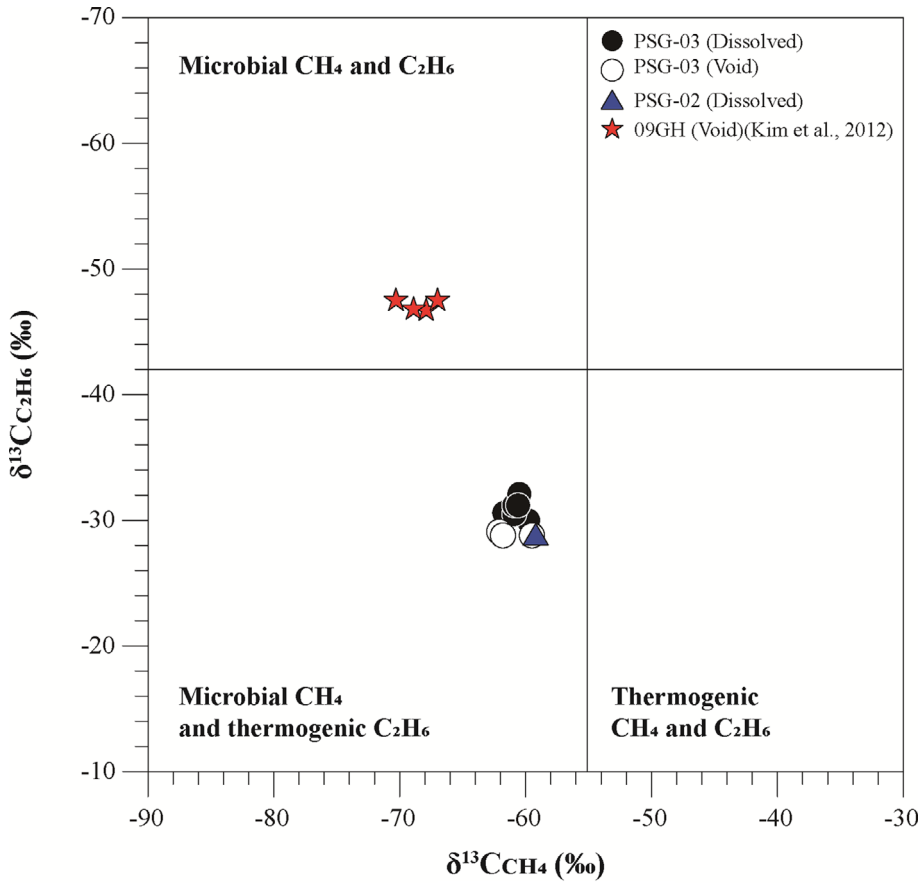

Fig. 9. $\delta^{13}C_{CH4}$ vs. $\delta^{13}C_{C2H6}$ plots obtained for dissolved and the void gases from the Pohang Basin and the void gas sampled from the 09GH expedition in the Ulleung Basin, East Sea (adapted from Milkov et al., 2005).

the oxidation of CH_4 by aerobic and/or anaerobic bacteria, which selectively removes ^{12}C and thus increases $\delta^{13}C$ (Whiticar et al., 1986) to values that can be similar to those of thermogenic CH_4. Groundwater flows into the Pohang Basin to form an aquifer (Korea Water Resources Corporation, 2003), which is an important condition for methane oxidation. Since oxidation of CH_4 is a microbial metabolic process in which CH_4 is oxidized to CO_2, preferential consumption of $^{12}CH_4$ leads to CO_2 fraction that is highly enriched in ^{12}C (Bernard et al., 1978; Whiticar, 1999; Whitical and Elvert, 2001). As a result, the difference in the isotopic composition of CO_2 and CH_4 ($\delta^{13}C_{CO2} - \delta^{13}C_{CH4}$) remains consistent for CH_4 production, but strongly decreases for CH_4 oxidation (Whiticar, 1999; Pohlman et al., 2009; Kim et al., 2012). In this study, the difference in $\delta^{13}C_{CO2}$ and $\delta^{13}C_{CH4}$ show consistent value in dissolved gas (37–49), but gradually decrease to the north in void gas (3–62) (Fig. 10). A cross-plot of $\delta^{13}C_{CO2}$ and $\delta^{13}C_{CH4}$ suggests that CH_4 is affected by microbial oxidation, or that it contains a ^{13}C-enriched fraction from a thermogenic source (Kim et al., 2012). Because oxidation by bacteria preferentially consumes CH_4 dissolved in water, methane oxidation modulates the amount of dissolved methane and affects the isotopic signature. However, there is no isotopic signature for the effect of methane oxidation in dissolved methane (Fig. 10a). Besides, if the oxidizing bacteria increase the $\delta^{13}C$ values toward the northern part of the study area, the CH_4 content should decrease in the same direction. However, the CH_4 content is the highest for PSG-02, located in the south, and for PSG-03, located in the north. In other words, no change in CH_4 content due to oxidation is observed. Therefore, the influence of microbial oxidation on $\delta^{13}C_{CH4}$ over time is not significant for the Pohang Basin.

Another factor that may influence $\delta^{13}C$ is secondary biogenic CH_4, which is generated when hydrocarbons (oil or gas) are expelled from organic-rich shales, migrate toward shallower, cooler, and more porous formations inhabited by methanogens, and are degraded within the oil-water or water-gas transition zones. Thus, the $\delta^{13}C$ values of secondary biogenic gas can exceed those of primary biogenic gas (–40‰ to –80‰) (Scott et al., 1994; Tao et al., 2005). In terms of geological characteristics, the Pohang Basin has favorable conditions (OM-rich shales, shallow depth resulting from tectonic uplift, ground water flow, and optimal temperature) for the generation of secondary biogenic gas. However, according to the lipid biomarker study of D.H.

https://doi.org/10.1007/s12303-021-0035-1

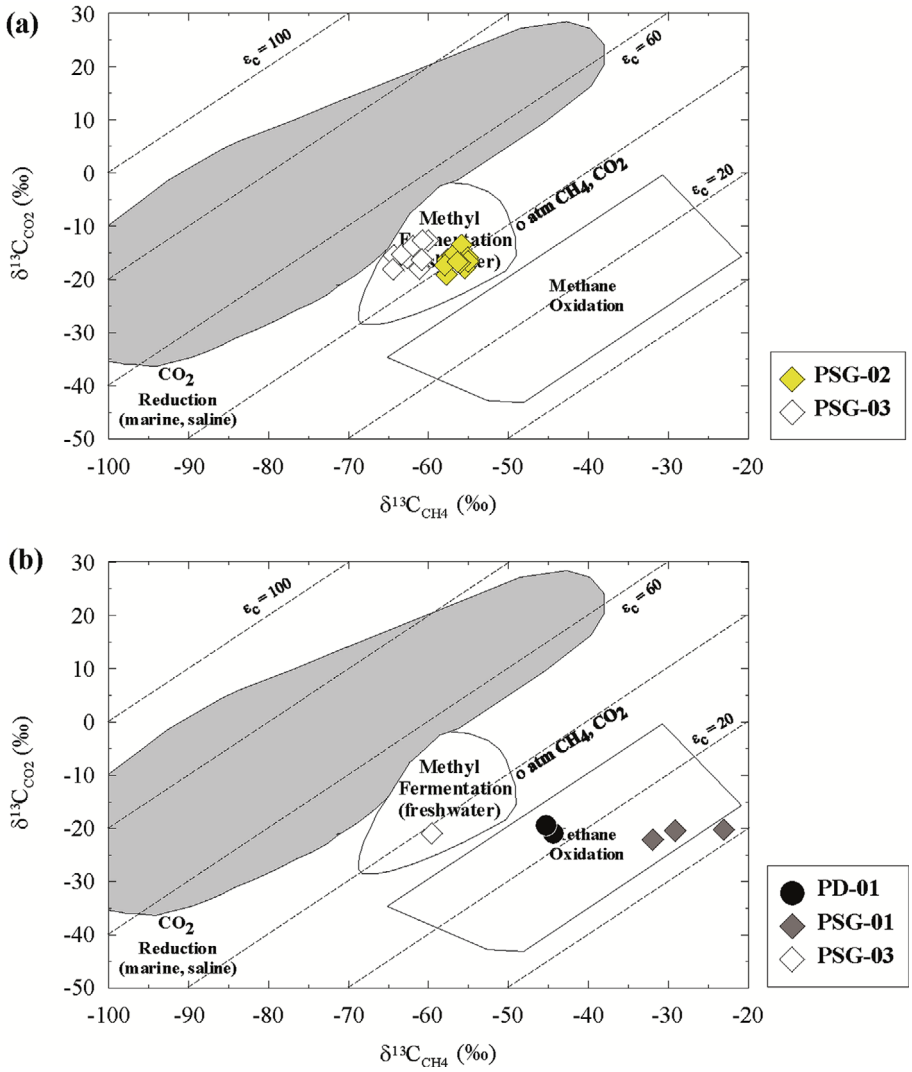

Fig. 10. $\delta^{13}C_{CH4}$ vs. $\delta^{13}C_{CO2}$ plots obtained for (a) the dissolved gas and (b) the void gas from the Pohang Basin with isotopic fractionation lines (adapted from Whiticar, 1999; Pohlman et al., 2009; Kim et al., 2012).

Lee et al. (unpublished manuscript), no specific lipid biomarkers (e.g., isoprenoid dialkyl glycerol diethers; archaeol and hydroxyarchaeol) derived from methanogens are detected in any core samples. This suggests that the generation of secondary biogenic gas in this system is negligible and is unlikely to affect $\delta^{13}C$.

The impacts of thermogenic CH_4 on $\delta^{13}C$ must be considered as well. In general, thermogenic CH_4 derived from the subsurface thermal defragmentation of kerogen and/or hydrocarbons ranges from –50‰ to –20‰, with values between –50‰ and –60‰ often attributed to the mixing of thermal and microbial CH_4 (Whiticar, 1999). Herein, the $\delta^{13}C$ of dissolved CH_4 is mostly in the range expected for mixing, and the values of void CH_4 are close to those expected for a thermogenic source. To determine the exact gas origin, we compared $\delta^{13}C_{C2H6}$ for the dissolved and void gas samples. The values of $\delta^{13}C_{CH4}$ ranged from –32.1‰ to –28.9‰ for the dissolved gas and from –29.1‰ to –28.8‰ for the void gas, indicating a thermal origin. The obtained $\delta^{13}C_{C2H6}$ values shows not only the features of thermogenic C_2H_6, but also mixed features of biogenic CH_4 and thermogenic C_2H_6. Rice (1993) suggested that the coexistence of ^{13}C-rich C_2H_6 ($-28‰ < \delta^{13}C_{C2H6} < -24‰$) and ^{13}C-depleted CH_4 ($\delta^{13}C_{CH4} < -55‰$) resulted from a mixture of biogenic and thermogenic origins. Although the difference between the $\delta^{13}C_{CH4}$ values of the dissolved and void gases are difficult to explain, they clearly exceeded those expected for a biological source and could only be rationalized by the influence of thermogenic sources. Migration of thermogenic gas from the deep basin and mixing with biogenic gas generated along the northern margin account for this pattern. Therefore, the carbon isotopic compositions of the dissolved and void gases have demonstrated a mixed gas characteristic in the Pohang Basin.

Table 5. Geochemical data from global biogenic gas system

Location	Biogenic gas system	Reservoir age	Reservoir Depth (m)	Gas Type	$\delta^{13}C_{CH4}$ (‰)	δD_{CH4} (‰)	$\delta^{13}C_{CO2}$ (‰)	OM contents (wt%)	OM type	References
Pohang Basin /Korea	Early-generation	Tertiary	–	Dissolved	−64.2 – −51.5	−227 – −206	−20.7 – −12.6	1.1 – 2.9	Type II	this study
				Void	−62.1 – −22.9	−219 – −189	−22.3 – −19.6			
Eastern Denver Basin/USA	Early-generation	Late Cretaceous	250–850	Void	−65.0 – −55.0	n.d.	n.d.	1.0 – 5.8	Type II	Rice (1984)
Southeastern Alberta Basin/ Canada	Early-generation	Cretaceous	300–1000	Void	−60.0 – −68.3	n.d.	n.d.	n.d.	Type III	Ridgley et al. (1999)
Northern Michigan Basin/USA	Late-generation	Late Devonian	600	Void	−56.0 – −47.0	−260 – −207	−23.2 – −13.1	0.5 – 24	Type I, II, III	Martini et al. (1998)
Powder River basin/USA	Late-generation	Tertiary	110–122	Void	−53.8 – −56.5	−307 – −333	n.d.	n.d.	Type III	Rice (1993)

5.4. Shallow Biogenic Gas System in the Pohang Basin

In general, unconventional shallow biogenic gas can be generated in two distinct systems, namely the early- and late-generation systems (see Introduction). Early-generation systems are exemplified by the southeastern Alberta Basin and the eastern Denver Basin, and late-generation systems are represented by the Powder River Basin and the northern Michigan Basin (Table 5). For both systems, the gas is predominantly CH_4 and is associated with thermally immature source rocks. Biogenic gas in the eastern Denver Basin (Niobrara gas play) was produced early in the burial history, and was generated by the microbial degradation of OM in an anaerobic environment (Rice, 1984). An organic-rich layer of kerogen type II provided an adequate source for the gas (Rice, 1984). Shale containing bentonite beds in the lower part served as a seal for the gas after its accumulation (Rice, 1984). $\delta^{13}C_{CH4}$ values in the range –65‰ to –55‰ support a biological origin of the shallow gas. On the other hand, biogenic gas in the northern Michigan Basin (Antrim gas play) accumulated in a shallow basin over geologically brief time periods (Martini et al., 1998). In particular, a well-developed fracture system provided conduits for freshwater transport, resulting in widespread microbial communities (Martini et al., 1998). The Antrim shale gas exhibits relatively high $\delta^{13}C_{CH4}$ values ranging from –56‰ to –47‰. These high isotopic signatures result from mixing of biogenic gas and thermogenic gas that migrated up from the deep basin (Martini et al., 1998).

The shallow gas in the Pohang Basin is interpreted to be of biological origin due to its chemical and isotopic composition and T_{max} values indicating that tertiary rocks in the study area are mostly immature. Nevertheless, it is noted that the $\delta^{13}C_{CH4}$ values generally exceeded the values of the recent biogenic gas system located in the Ulleung Basin (–70‰ to –80‰, Choi et al., 2013). These relatively high isotopic values are considered to represent a mixture of biogenic and thermogenic gas that has migrated from the northeastern deep basin, similar to the Antrim gas system. However, while the microbial community is widely distributed in the Antrim gas system, no biomarker evidence for methanogenic microbes was found in the Pohang Basin. The isotopic characteristics of the hydrocarbon gas in the Pohang Basin are similar to those of the Antrim gas; however, it was determined that it is not a late-generation system. Rather, it is believed that the gas generated in the organic-rich layer early in the burial history was sealed by the mudstone, similar to the Niobrara gas system. The $\delta^{13}C$ data also support the hypothesis that the gas is old and began to form and accumulate soon after deposition (Rice, 1975; Rice and Claypool, 1981). Therefore, the biogenic gas system in the Miocene Pohang Basin is an early-generation system.

6. CONCLUSIONS

The mechanism of shallow biogenic gas generation in the Miocene Pohang Basin was studied by analyzing the OM and hydrocarbon gas extracted from five wells (PD-01, PD-02, PSG-01, PSG-02, and PSG-03). The main conclusions are presented below.

1. The OM content was found to range from 1.10 to 2.87 wt%, averaging at 1.85 wt%. The modified van Krevelen diagram and $\delta^{13}C$ values are indicative of type II/III marine OM. The measured thermal maturity is below 438 °C, implying an immature stage. These results suggest that the Pohang Basin contains high-quality source rocks for biogenic gas production.

2. The molecular signatures of the dissolved and void gases show that CH_4 is the dominant hydrocarbon in all cases, with C_2H_6 and C_3H_8 detected in minor amounts. The $\delta^{13}C_{CH4}$ and δD_{CH4} values of the dissolved gas are generally less than –51.5‰ and –206‰, respectively, indicating a biogenic (CO_2 reduction) origin. However, the $\delta^{13}C_{CH4}$ values (< 22.9‰) observed for the northern part of the basin support the influence of thermogenic gas that migrated from the thermally-matured deep basin.

3. The hydrocarbon gases of the Pohang Basin are a mixture of biogenic and migrated thermogenic gases, as supported by

https://doi.org/10.1007/s12303-021-0035-1

the relationship between $\delta^{13}C_{CH4}$ and $\delta^{13}C_{C2H6}$.

4. The geochemical data indicate that the unconventional shallow biogenic gas system of the Pohang Basin is an early-generation system, as supported by $\delta^{13}C_{CH4}$ values exceeding those of a recent biogenic gas system and the absence of methanogens in the studied cores.

5. This study provides new insights into the shallow biogenic gas system in the Pohang Basin using the geochemical compositions of OM and hydrocarbon gas. The geochemical data are essential for understanding this shallow gas reserve. This is critical data for the development of future exploration strategies and long-term recoverable reserve estimates of natural gas.

ACKNOWLEDGMENTS

This work was supported by the Korea Institute of Energy Technology Evaluation and Planning (KETEP) and the Ministry of Trade, Industry & Energy (MOTIE) of the Republic of Korea (No. 20172510102160), and the gas hydrate R&D project of Ministry of Trade, Industry and Energy, Korea (21-1143-2).

REFERENCES

Bernard, B.B., Brooks, J.M., and Sackett, W.M., 1978, Light hydrocarbons in recent Texas continental shelf and slope sediments. Journal of Geophysical Research, 83, 4053–4061.

Choi, J., Kim, J.-H., Park, S., and Kang, N.K., 2019, A study on the gas and organic geochemical characteristics in the Pohang Basin. 2019 Joint Conference of the Geological Science and Technology of Korea (Abstract), Jeju, Apr. 17–19, p. 13.

Choi, J., Kim, J.-H., Torres, M.E., Hong, W.-H., Lee, J.-W., Yi, B.-Y., Bahk, J.-J., and Lee, K.E., 2013, Gas origin and migration in the Ulleung Basin, East Sea; results from the second Ulleung Basin gas hydrate drilling expedition (UBGH2). Marine and Petroleum Geology, 47, 113–124.

Chough, S.K., Hwang, I.G., and Choe, M.Y., 1990, The Miocene Doumsan fan-delta, southeast Korea: a composite fan-delta system in back-arc margin. Journal of Sedimentary Petrology, 60, 445–455. https://doi.org/10.1306/212F91BA-2B24-11D7-8648000102C1865D

Claypool, G.E. and Kaplan, I.R., 1974, The origin and distribution of methane in sediments. In: Kaplan, I.R. (ed.), Natural Gases in Marine Sediments. Marine Science, Springer, Boston, 3, p. 99–139. https://doi.org/10.1007/978-1-4684-2757-8_8

Claypool, G.E. and Kvenvolden, K.A., 1983, Methane and other hydrocarbon gases in marine sediments. Annual Review of Earth and Planetary Sciences, 11, 299–327. https://doi.org/10.1146/annurev.ea.11.050183.001503

Espitalié, J., Deroo, G., and Marquis, F., 1985, La pyrolyse Rock-Eval et ses applications. Deuxième partie. Oil & Gas Science and Technology – Revue de l'IFP, 40, 755–784. (in French) https://doi.org/10.2516/ogst:1985045

Hwang, I.G., 1993, Fan-delta systems in the Pohang Basin (Miocene), SE Korea. Ph.D. Thesis, Seoul National University, Seoul, Korea, 923 p.

Hwang, I.G., Chough, S.K., Hong, S.W., and Choe, M.Y., 1995, Controls and evolution of fan delta systems in the Miocene Pohang Basin, SE Korea. Sedimentary Geology, 98, 147–179.

Kang, N.K., Hwang, I.G., Ahn, T., Choi, J., Lee, T., and Lee, H.S., 2019, Overview of research and exploration to study the characteristics of the shallow gas field reservoir in Daejam-dong, Pohang. 2019 Joint Conference of the Geological Science and Technology of Korea (Abstract), Jeju, Apr. 17–19, p. 11.

Kang, N.K., Hwang, I.G., An, T.W., Choi, J., Lee, T.H., and Lee, H.S., 2019, Overview of reservoir characterization of onshore shallow gas system in Daejam-dong in Pohang. 2019 Joint Conference of the Geological Science and Technology of Korea (Abstract), Jeju, Apr. 17–19, p. 11.

Kim, B.K., 1965, The stratigraphic and paleontologic studies on the Tertiary (Miocene) of the Pohang area, Korea. Seoul National University Journal, Science and Technology Series, 15, 32–121.

Kim, J.-H., Park, M.H., Chun, J.H., and Lee, J.Y., 2011, Molecular and isotopic signatures in sediments and gas hydrate of the central/southwestern Ulleung Basin: high alkalinity escape fuelled by biogenically sourced methane. Geo-Marine Letters, 31, 37–49.

Kim, J.-H., Torres, M.E., Choi, J.Y., Bahk, J.J., Park, M.H., and Hong, W.L., 2012, Inferences on gas transport based on molecular and isotopic signatures of gases at acoustic chimneys and background sites in the Ulleung Basin. Organic Geochemistry, 43, 26–38.

Korea Water Resources Corporation, 2003, Pohang area groundwater basic survey report. GOVP1200414638, Korea Water Resources Corporation, Daejeon, 1040 p.

Lafargue, E. Marquis, F., and Pillot, D., 1998, Rock-Eval 6 applications in hydrocarbon exploration, production, and soil contamination studies. Revue de l'Institut Francais du Petrole, 53, 421–437.

Lamb, A.L., Wilson, G.P., and Leng, M.J., 2006, A review of coastal palaeoclimate and relative sea-level reconstructions using $\delta^{13}C$ and C/N ratios in organic material. Earth-Science Reviews, 75, 29–57.

Li, Y.-L. and Lin, C.-M., 2010, Exploration methods for late Quaternary shallow biogenic gas reservoirs in the Hangzhou Bay area, eastern China. American Association of Petroleum Geologists Bulletin, 94, 1741–1759.

Martini, A.M., Budai, J.M., Walter, L.M., and Schoell, M., 1996, Microbial generation of economic accumulations of methane within a shallow organic-rich shale. Nature, 383, 155–158.

Martini, A.M., Walter, L.M., Budai, J.M., Ku, T.C.W., Kaiser, C.J., and Schoell, M., 1998, Genetic and temporal relations between formation waters and biogenic methane—Upper Devonian Antrim Shale, Michigan basin, USA. Geochimica et Cosmochimica Acta, 62, 1699–1720.

Milkov, A.V., Claypool, G.E., Lee, Y.-J., and Sassen, R., 2005, Gas hydrate systems at Hydrate Ridge offshore Oregon inferred from molecular and isotopic properties of hydrate-bound and void gases. Geochimica et Cosmochimica Acta, 69, 1007–1026.

Pang, X., Zhao, W., Su, A., and Li, S., 2005, Geochemistry and origin of the giant Quaternary shallow gas accumulations in the eastern Qaidam Basin, NW China. Organic Geochemistry, 36, 1636–1649.

Pape, T., Bahr, A., Rethemeyer, J., Kessler, J.D., Sahling, H., Hinrichs,

K.-U., Klapp, S.A., Reeburgh, W.S., and Bohrmann, G., 2010, Molecular and isotopic partitioning of low molecular-weight hydrocarbons during migration and gas hydrate precipitation in deposits of a high-flux seepage site. Chemical Geology, 269, 350–363.

Pimmel, A. and Claypool, G., 2001, Introduction to shipboard organic geochemistry on the JOIDES resolution. ODP Technical Note, Ocean Drilling Program, Texas A&M University, College Station, 30, 29 p. https://doi.org/10.2973/odp.tn.30.2001

Pohlman, J.W., Kaneko, M., Heuer, V.B., Coffin, R.B., and Whiticar, M., 2009, Methane sources and production in the northern Cascadia margin gas hydrate system. Earth and Planetary Science Letters, 287, 504–512. https://doi.org/10.1016/j.epsl.2009.08.037

Rice, D.D., 1975, Origin of and conditions for shallow accumulations of natural gas. in Wyoming Geological Association. 27th Annual Field Conference on Geology and Mineral Resources of the Bighorn Basin, Wyoming Geological Association Guidebook, p. 267–271.

Rice, D.D., 1984, Occurrence of indigenous biogenic gas in organic-rich, immature chalks of Late Cretaceous age, eastern Denver Basin. In: Palacas, J.G. (ed.), Petroleum Geochemistry and Source Rock Potential of Carbonate Rocks. AAPG Studies in Geology, The American Association of Petroleum Geologists, Tulsa, 18, p. 135–150.

Rice, D.D., 1993, Biogenic gas: controls, habitats, and resource potential. In: Howell, D.G. (ed.), The Future of Energy Gases. USGS Professional Paper, U.S. Geological Survey, Reston, 1570, p. 583–606. https://www.osti.gov/biblio/6814498 [Accessed on 30 October 2021].

Rice, D.D. and Claypool, G.E., 1981, Generation, accumulation, and resource potential of biogenic gas. American Association of Petroleum Geologists Bulletin, 65, 5–25.

Rice, D.D. and Shurr, G.W., 1980, Shallow low-permeability reservoirs of northern Great Plains—assessment of their natural gas resources. American Association of Petroleum Geologists Bulletin, 64, 969–987.

Ridgley, J.L., Hester, T.C., Condon, S.M., Anna, L.O., Rowan, E.L., Cook, T., and Lillis, P.G., 1999, Re-evaluation of the shallow biogenic gas accumulation, northern Great Plains, USA—is the similar gas accumulation in southeastern Alberta and southwestern Saskatchewan a good analog? Saskatchewan Energy and Mines Miscellaneous Report, Saskatchewan Geological Survey, 99-4.1, p. 64–78.

Scott, A.R., Kaiser, W.R., and Ayers Jr., W.B., 1994, Thermogenic and secondary biogenic gases, San Juan basin, Colorado and New Mexico—implications for coalbed gas productivity. American Association of Petroleum Geologists Bulletin, 78, 1186–1209.

Shurr, G.W., 2008, Shallow biogenic gas in Cretaceous shale on the eastern margin of the Williston Basin. In: Hill, D., Lillis, P., and Curtis, J. (eds.), Gas Shale in the Rocky Mountains and Beyond. Rocky Mountain Association of Geologists 2008 Guidebook CD, p. 176–198.

Shurr, G.W. and Ridgley, J.L., 2002, Unconventional shallow biogenic gas systems. American Association of Petroleum Geologists Bulletin, 86, 1939–1969.

Sohn, Y.K. and Son, M., 2004, Synrift stratigraphic geometry in a transfer zone coarse-grained delta complex, Miocene Pohang Basin, SE Korea. Sedimentology, 51, 1387–1408.

Tao, M., Wang, W., Xie, G., Li, J., Wang, Y., Zhang, X., Zhang, H., Shi, B., and Gao, B., 2005, Secondary biogenic coalbed gas in some coal fields of China. Chinese Science Bulletin, 50, 24–29.

Waples, D.W., 1985, Geochemistry in Petroleum Exploration. Reidel Publishing Company, Boston, 232 p.

Whiticar, M.J., 1999, Carbon and hydrogen isotope systematics of bacterial formation and oxidation of methane. Chemical Geology, 161, 291–314.

Whiticar, M.J. and Elvert, M.E., 2001, Organic geochemistry of Saanich Inlet, BC, during the Holocene as revealed by Ocean Drilling Program Leg 169S. Marine Geology, 174, 249–271.

Whiticar, M.J., Faber, E., and Schoell, M., 1986, Biogenic methane formation in marine and freshwater environments: CO_2 reduction vs. acetate fermentation-isotope evidence. Geochimica et Cosmochimica Acta, 50, 693–709.

Yoon, S., 1975, Geology and paleontology of the Tertiary Pohang Basin, Pohang district, Korea, Part I. Geology. Journal of Geological Society of Korea, 2, 187–214.

Yoon, S.H. and Chough, S.K., 1995, Regional strike slip in the eastern continental margin of Korea and its tectonic implications for the evolution of Ulleung Basin, East Sea (Sea of Japan). Geological Society of America Bulletin, 107, 83–97.

Yun, H., 1986, Emended stratigraphy of the Miocene Formation in the Pohang Basin, Part I. Journal of Paleontological Society of Korea, 2, 54–69.

https://doi.org/10.1007/s12303-021-0035-1